Reprinted from THE REVIEW OF SCIENTIFIC INSTRUMENTS, Vol. 39, No. 7, 1029–1035, July 1968
Printed in U. S. A.

Discharge Mechanism in Gases in the Subnanosecond Region

JUAN T. D'ALESSIO AND HILDA LANZA
Departamento de Fisica Atómica y Molecular, Dirección de Investigaciones, Comisión National de Energia Atómica, Buenos Aires, Argentina

(Received 26 July 1967; and in final form, 25 March 1968)

The mechanisms of spark generation which produce luminous and electric pulses of the order of subnanoseconds in a gas at a high pressure are analyzed. The classical mechanisms, which account for regenerative processes initiated by the photons produced during the avalanches of electrons, cannot explain the generation of 10^{11} electrons in 0.3 nsec, which were experimentally detected when using our generator. In this work, the experimental results are interpreted by means of a model which considers the equilibrium surface shape of the liquid as the resultant of an increase in the field near the electrodes up to 10^{9}–10^{10} V/cm (the surface shape is determined by the superimposed effect of the electric field and the surface tension). With a field of this magnitude, electrons are produced at the cathode in numbers large enough to explain the experimental results. In agreement with the model proposed, pulses of 10^{-10} sec duration can only be obtained with liquid electrodes in gases at a high pressure.

INTRODUCTION

To study the decay times of very fast scintillators and other processes associated with them (energy transfer mechanisms in liquid or solid media, quenching effects, eximer formation, etc.), it is necessary to use pulse generators of extremely short duration, in the region of nanoseconds and subnanoseconds.

Visible and ultraviolet light generators are particularly interesting, as excitation by means of these radiations leads to simpler interpretation of the results due to the almost total absence of secondary processes; also the use of narrow band optical filters allows a high excitation selectivity which is difficult to obtain in other regions of the energy spectrum. Thus, it is of great interest to produce pulses of extremely short duration which combine a condition of high luminous intensity with the possibility of a high repetition rate and high reproducibility in shape and in amplitude.

PULSE GENERATORS

Earlier works[1,2] describe spark generators which had electrodes wetted by mercury and were filled with hydrogen gas at high pressure to produce luminous and electric pulses.[3]

The analysis of these generators, studied by the authors and Kerns *et al.*,[4] leads to the conclusion that good quality pulses of less than 1 nsec duration can be obtained only under the following conditions: (a) high pressure (of the order of 30 atm), (b) electrodes wetted by mercury or of pure mercury, and (c) coaxial assembly.

With respect to point (a), for each electrode profile there exists a critical pressure; below this critical value, the amplitude, duration and fluctuation of the pulse become very unsatisfactory.

With respect to point (b), the fluctuation is nearly 20 times greater and the duration is higher than 1 nsec if solid electrodes are used. Also, the electrodes wetted by mercury have an almost unlimited life.

With respect to point (c), if precautions are not taken in the assembly of the generator, electrical reflections and oscillations damage the quality of the pulse.

ELECTRICAL MODEL

In order to obtain the time necessary for a gas to reach its state of highest electrical conductivity with greater precision, the pulse generator was considered as a variable resistance $r=r(t)$ and the equivalent circuit was analyzed using the curve $i=i(t)$ obtained at point A (Fig. 1).

Figure 1 shows the generator circuit, Fig. 2 shows the equivalent circuit and Fig. 3 the curve $i=i(t)$—calculated from $v=v(t)$—obtained at point A of the 50 Ω resistance with a sampling oscilloscope (Hewlett–Packard model 185 A, risetime 0.1 nsec).

If it were also possible to measure $v=v(t)$ at point B, $r=r(t)$ could have been calculated. This measurement cannot be made without altering the electrical character-

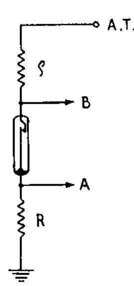

FIG. 1. Generator circuit.

[1] J. T. D'Alessio, P. K. Ludwig, and M. Burton, Rev. Sci. Instr. 35, 1105 (1964).

[2] J. T. D'Alessio and P. K. Ludwig, IEEE Trans. Nucl. Sci. NS-12, No. 1, 351 (1965).

[3] A luminous pulse is produced synchronously with an electrical pulse. Several authors had estimated theoretically that the time difference between both pulses is lower than 10^{-13} sec. The resolution of available experimental methods is not high enough to confirm this estimation. As a result of this work it is concluded that the time difference is not greater than 10^{-11} sec, but as this value is the resolution limit of the instruments used, it is difficult to attach much importance to this figure.

[4] O. A. Kerns, F. Kirsten, and G. Cox, UCRL, 8277 (1958).

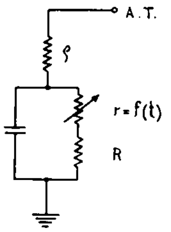

FIG. 2. Equivalent circuit of the generator.

istics of the discharge circuit, since the capacity of the generator is very small (~5 pF).

The analysis of the circuit leads to the following differential equation in r:

$$A\ddot{r}+B\dot{r}+Cr+D=0$$

where

$$A=i,$$

$$B=2(di/dt)+(i/cR),$$

$$C=\frac{d^2i}{dt^2}+\frac{1}{cR}\cdot\frac{di}{dt},$$

and

$$D=R\frac{d^2i}{dt^2}+\frac{\rho}{c}\cdot\frac{di}{dt}.$$

Since the coefficients A, B, C, and D contain terms which are time dependent $[i, (di/dt), (d^2i/dt^2)]$, r was calculated numerically after obtaining i, di/dt and d^2i/dt^2 graphically.

In the calculation it was supposed that all the energy stored in the capacitor c was dissipated as heat in the resistances $[R$ and $r=r(t)]$. This implies that the energy which was transformed into light was negligible. This assumption is justified on the basis of photometric measurements by Kerns and his collaborators,[4] and from the emission spectrum of the generator used. The latter was corrected for the absorption of the glass and the spectrophotometer response. Thus the number of photons emitted

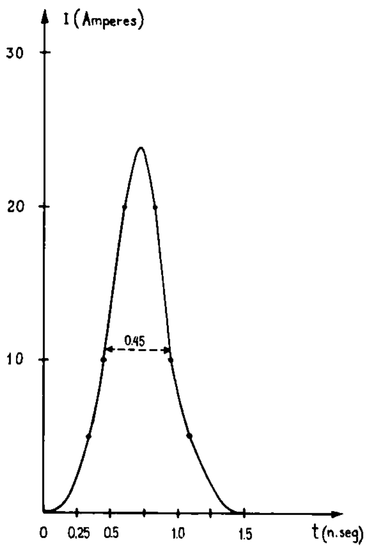

FIG. 3. Electric pulse obtained through resistance R.

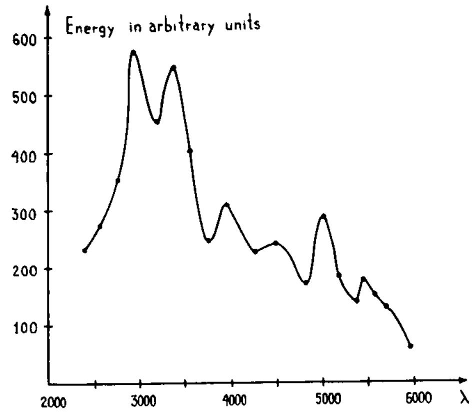

FIG. 4. Spectrum of the luminous pulse.

for each pulse was estimated to be between 10^7 and 10^8 and their average energy was 4 eV (~3200 Å) (see Fig. 4). The total light energy involved was between 10^{-12} and 10^{-11} J.

On the other hand, the electrical energy dissipated at the resistance R is of the order of 10^{-5} J which means that the luminous yield is very low.

Figure 5 shows $r=r(t)$. It is concluded that (a) the resistance drops from 10^8 to $10^2\,\Omega$ in 0.3 nsec. This is the time in which the gas changes from a state of very low conductivity to one of the highest ionization. This value is of singular importance in the analysis of the possible spark formation mechanism. (b) After this, the resistance drops much more slowly, maintaining its value at about $10^2\,\Omega$. This relatively high resistance is explained by a narrow spark section. The beam diameter has been estimated to be a few microns, on the basis of the diffusion values and by comparison with the resistance of other types of sparks. The direct microscopical observation confirms the order of magnitude.

From the experimental curve $v=f(t)$, it has been estimated that 10^{11} to 10^{12} electrons are emitted in each pulse.

SPARK FORMATION MECHANISM

In order to explain the mechanism by which a channel of high conductivity is formed in a gas, several regenerative processes produced after the first avalanche have to be taken into account.

The main regenerative processes are (a) photoelectron production at the cathode by photons generated during the avalanches, (b) photoelectron production in the gas by photons of the same origin, (c) liberation of secondary electrons at the cathode by collision with positive ions, (d) ionization of atoms or molecules in an excited metastable state (by collision with other atoms or molecules or by collisions of the second kind with the cathode), and (e) ionization of metastable atoms or molecules by photons generated in previous avalanches.

Some competitive processes of secondary electron emission are photon absorption, metastable atom or molecule de-excitation without ionization, and the recombination of ions with electrons in the gas or at the cathode. All of these processes are associated with characteristic time intervals. The speed of the regenerative process is of great interest since the duration of the electrical and luminous pulses depends on it. These time intervals depend on the pressure and nature of the gas and on the intensity and distribution of the electrical field between the electrodes.

An analysis of the time interval corresponding to each process leads to the following conclusions (related to the production of pulses of tenths of a nanosecond):

(1) Considering the drift velocity of the avalanche and with electrodes separated by a distance of 0.4–0.5 mm, the time in which the front of the avalanche reaches the anode is of the order of 0.1 nsec. As the main bulk of the secondary electrons and photons is produced near the anode,[5] the photoelectrons produced at the cathode should have a delay of this order of magnitude (0.1 nsec). This is why it is improbable that the contribution of successive avalanches to the main discharge is important in 0.3 nsec.

(2) The contribution of electrons produced at the cathode by collision of ions is negligible due to the low mobilities of the heavy ions. A simple calculation shows that the time involved is much longer than that being studied in this work.

(3) The reproduction of secondary electrons by photons in the gas can be important only near the anode, because the effective photons of high energy (far ultraviolet) are strongly absorbed by the gas at high pressure. In this case, the multiplication of these electrons is low, due to the short path to the anode. There is no doubt that this process plays an important part in the formation of coronas in gases at lower pressures. But, when the pressure is increased, it can be observed that the corona becomes compressed towards the electrodes and vanishes at a sufficiently high pressure. The contribution of this process to the spark formation must be unimportant under the experimental conditions used in this work.

(4) The same objection, as used in the case of emission of ions or photons, may be applied to the contribution of regenerative processes by metastable atoms or molecules.[6]

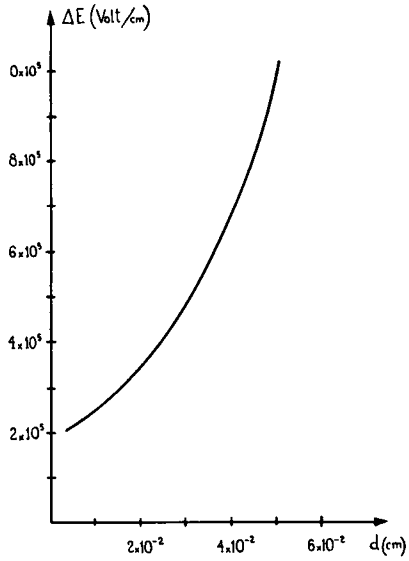

FIG. 6. Electric field dependence on the distance to electrodes.

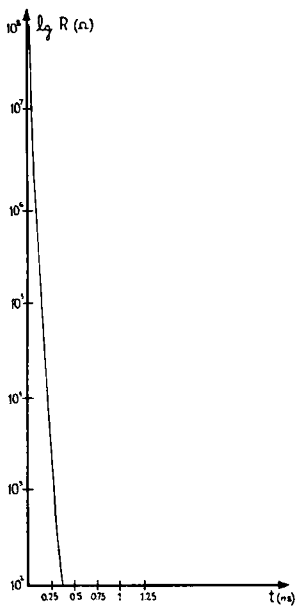

FIG. 5. Dependence on time of the internal resistance of the generator.

The difficulty of interpreting the production of about 10^{11} electrons in 0.3 nsec can be avoided if we accept the simultaneous production of a great number of avalanches without much interference between them; an estimation of the number of these avalanches shows that the cathode should emit about 10^4 electrons in each pulse. In order to consider this possibility, the probable cathodic emission must be taken into account.

Cathodic Field Emission

For the computation of the field between the electrodes with a point–plane geometry, the field equations have been applied near the axis with the boundary conditions suitable for the electrode surface.

A first approximate calculation showed that the field decreases very quickly outside the axis, so in what follows only the field at the axis must be considered. Figure 6 shows the function $E=f(x)$ obtained for a gap of 0.4 mm, $V=10\,000$ V, and a radius of curvature of the point electrode of about 0.5 mm.

[5] 63% at a distance of $1/\alpha$ to the anode, in a homogeneous field (α=constant). In fact, it is higher because $\alpha=f(E)$ and, since the field is greater near the electrodes, α is larger.

[6] The possibility of regenerative processes previous to the spark cannot be disregarded if the electrical conductivity of the gas is very low.

The values of E vary from a minimum of 2×10^5 V/cm near the plane electrode, to a maximum of 10^6 V/cm near the point electrode. The corresponding values of E/p for $p=30$ atm are 9 and 44 V/cm and Torr respectively.

Similar results can be obtained using the equations developed by Fitzsimmons[7] for a hyperboloid of revolution. With the calculated value of E, the electronic emission can be calculated.

The current density of field emitted electrons at room temperature is given by the Fowler and Nordheim equation

$$J=\frac{2.54\times10^{-6}E^2\exp\{[-(6.83\times10^7\varphi^{\frac{3}{2}})/E]\,[3.79\times10^{-4}(E/\varphi)^{\frac{1}{2}}]\}}{\varphi\bar{t}^2[3.79\times10^{-4}(E/\varphi)^{\frac{1}{2}}]}$$

where φ is the work function in electron volts, $\bar{t}$ and r are tabulated functions for argument values between 0 and 1, $\bar{t}$ is practically equal to 1, and r has values shown in Table I. v has been calculated as a function of

$$y=[3.79\times10^{-4}(E/\varphi)^{\frac{1}{2}}].$$

Table II gives the density of electrons in amperes per square centimeter, seconds, and the total number of electrons emitted in each pulse (i.e., in 0.3 nsec). As can be seen from the table, the electron emission at the cathode—at room temperature—for fields of 10^6 V/cm, and a radius of curvature of 0.5 mm, is 4×10^{-99} electrons, that is, almost nonexistent.

Cosmic radiation electrons, ultraviolet light from the cathode or radioactivity of the materials, could explain the emission of the first electrons which start the avalanche, but not 10^4 simultaneous electrons as required here.

Another explanation would be to assume that the fields are much more intense than the one considered. Since $\alpha=f(E/p)$, avalanches could be produced with a multiplication factor of about 10^{11} electrons by one electron generated near the cathode.

The results obtained using electrodes wetted by mercury, or with mercury electrodes in a capillary tube, clearly show that liquid mercury plays a main role in the production of subnanosecond pulses, and with the characteristics previously noted.

These results are: (a) the pulse is shorter with mercury electrodes than with solid metals (nickel, tungsten, etc.); (b) the pulse shape is practically independent of the geometry of the electrodes (point-to-plane geometry was generally used, but, with two plane electrodes, pulses of similar characteristics were obtained provided the electrodes were wetted by mercury); and (c) even in the case of point-to-plane electrodes, polarity reversal does not affect the pulse quality nor its amplitude. On the other hand, the polarity and geometry of asymmetric solid electrodes have a great influence on the shape of the pulses. A less important observation is the formation of a thin layer of mercury on the walls of the generator after some hours of operation at a high rate, for example, 24 h at 3000 pulses/sec (about 2.6×10^8 pulses in 24 h).

TABLE I. v (parameter in the Fowler–Nordheim equation) vs y $[y=3.79\times10^{-4}(E/\varphi)^{\frac{1}{2}}]$.

y	v
0	1
0.1	0.982
0.2	0.937
0.3	0.872
0.4	0.789
0.5	0.690
0.6	0.577
0.7	0.450
0.8	0.312
0.9	0.161
1	0

Equilibrium Shapes of Mercury

The difficulties of establishing a satisfactory mechanism to explain an increase in the gas conductivity in 0.3 nsec and the results previously described, suggest the possibility that the true shape of the electrodes when the spark is produced is not the shape of the solid electrodes, but one resulting from the mercury that covers the electrodes which is influenced by the intense electric field.

An analysis of this shape shows that the true electric field in which the spark is produced is several orders of magnitude higher than the one previously supposed. This new field affects the electronic emission at the cathode and the avalanche multiplication.

In order to find the equilibrium shape of the mercury surface, the following three factors must be considered: (1) surface tension, (2) repulsion between charges on the same electrode, and (3) attraction between charges on different electrodes. The following equations apply:

$$\delta w_{\rm I}=\alpha\delta S \qquad (1)$$

TABLE II. Density and number of electrons emitted at the cathode vs E.

E (V/cm)	j (A/cm^2 sec)	N (electrons)
10^4	$40\times10^{-5.5\times10^4}$	negligible
10^5	4×10^{-103}	negligible
10^6	4×10^{-95}	4×10^{-99}
10^7	4×10^{-37}	4×10^{-41}
10^8	3×10^{15}	4×10^{11}
10^9	10^{104}	10^{100}

[7] K. E. Fitzsimmons, Phys. Rev. 61, 175 (1942).

where

$$\delta S = \int \left[\frac{\partial^2 \xi}{\partial x^2} + \frac{\partial^2 \xi}{\partial y^2} \right] d\xi dS,$$

δw = energy variation; α = surface tension; δS = change of surface; ξ = coordinate normal to the deformed surface.

The electrostatic pressure is $\sigma^2 dS/2\epsilon$, where σ is the surface charge density and ϵ the dielectric constant.

$$\delta w_{\mathrm{II}} = (\sigma^2/2\epsilon) dS d\xi. \quad (2)$$

Since the interaction energy between electrodes is qV, its differential is

$$\delta w_{\mathrm{III}} = \sigma dS dV + V d\sigma dS \quad (3)$$
$$= \sigma dS(\partial V/\partial \xi) d\xi + V(\partial \sigma/\partial \xi) d\xi dS.$$

In equilibrium $\sum \delta w_i = 0$. At the surface of the conductor $\sigma \epsilon E_N = -\epsilon(\partial V/\partial \xi)$, ($E_N$ is the normal field component). Then,

$$\frac{1}{2}\left(\frac{\partial V}{\partial \xi}\right)^2 + V\frac{\partial^2 V}{\partial \xi^2} + \frac{a}{E}\left[\frac{\partial^2 \xi}{\partial x^2} + \frac{\partial^2 \xi}{\partial y^2}\right] = 0.$$

Resolution of this equation gives the important result that the radius of curvature of the mercury drops, under the experimental conditions of the generator used ($d = 0.4$ mm, $V = 10\,000$ V), to 20–30 Å. Figure 7 shows the probable equilibrium shapes of the mercury electrodes with an increasing electric field (a to d); at e, a spark is formed.

The consequence of this surface deformation is the qualitative and quantitative change in the electric field. Figure 8 shows the approximate field shape for a radius of curvature of both electrodes of 25 Å. The following points are noted:

(a) The symmetry of the electric field is independent of the shape of the solid support of the mercury, which explains the observations (b) and (c) in the previous section.

(b) Near the electrodes, the field is greater, by several orders of magnitude (10^9–10^{10} V/cm), than that which should have been obtained with solid electrodes (Fig. 6), and E/p is of the order of 10^4–10^5 V/cm, Torr.

An immediate consequence of this large field intensification near the cathode is that the cathode field emission is greatly increased. From Table II it can be seen that there

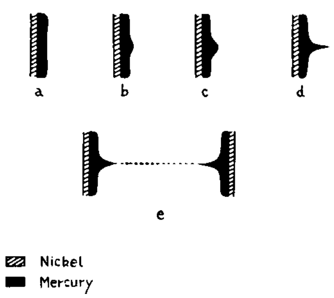

FIG. 7. Equilibrium shapes of the mercury surface when deformed by an electric field.

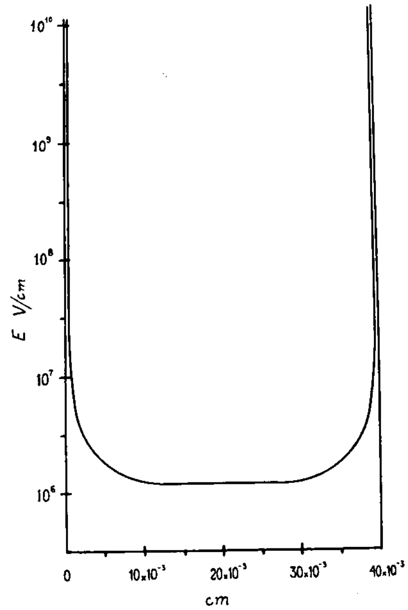

FIG. 8. Electric field dependence on the distance to electrodes when the mercury surface has adopted its equilibrium shape.

is an almost infinite field emission for these values of E/p.

This emission gives the required condition of a minimum of 10^4 simultaneous avalanches needed to explain the increase in the conductivity of the gas of more than five orders of magnitude in 0.3 nsec.

A further result of the increase in electric field strength with change in electron configuration is the rise in the values of α (Townsends' first coefficient), and with it, the multiplication of each avalanche.

There are no values of α (or of α/p) corresponding to values of E/p greater than 1000 V/cm, Torr. The curve shown in Fig. 9 was drawn from Halls' values for hydrogen[8] up to values of E/p near 10^3. It can be deduced from the form of the curve that the value of α/p should not increase much more than the limiting value[8] and the extrapolation for values of E/p from 10^4 to 10^5 must be verified experimentally.

Halls' values refer to hydrogen. In hydrogen contaminated with mercury, α grows because of the favorable effect of the metastable states of mercury on the ionization of the hydrogen. In order to establish the importance of this effect on the experimental condition of the generator used, it is necessary to study more carefully the processes occurring during the spark.

Neither can it be asserted that at high pressures α/p and E/p are the relevant parameters, because no previous experiments have been carried out with pressures greater than 1 atm.

In order to estimate the multiplication factor of each avalanche, a value of α/p of $75 \cdot 1$/cm, Torr has been adopted, that is, for $p = 30$ atm, $1.7 \times 10^5 \cdot 1$/cm for regions of high field intensity. It should be understood that mean-

[8] L. B. Loeb, *Basic Processes of Gaseous Electronics* (University of California Press, 1955), Chap. XIII.

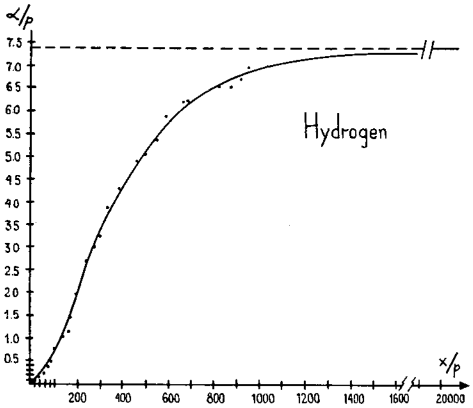

FIG. 9. α/p (α is Townsend's first coefficient) vs E/p, for hydrogen.

ing can be attached only to the *order* of magnitude. The electric field between the electrodes is not homogeneous; therefore, in order to make calculations, the gap has been divided into zones and each of the zones is considered to have a homogeneous field. Table III summarizes the results. As can be seen from the table, this estimation leads to the conclusion that one electron emitted by the cathode gives rise to 10^{21} electrons. This value is several orders of magnitude greater than that obtained experimentally in each pulse ($\sim 10^{11}$) in the electrical circuit of the generator.

The following curious situation thus arises: due to the deformations of the liquid surfaces, the electric field is increased, and this gives rise to cathodic emission and the production of avalanches with a high multiplication factor. In this way, the production of a large amount of electrons in tenths of a nanosecond can be explained.

These results do not contradict the experimental evidence because the limitation of the external current (or the number of electrons that go from the anode and return to the cathode), is given by the amount of energy stored in the condenser c (the capacity of the generator electrodes and the distributed capacitances), at the spark voltage V_f. In fact, as the electrons neutralize the positive charges of the anode, the field in the neighborhood of the anode is reduced to zero; that is, the area behind the curve of $i=f(t)$ of the electric pulse depends on the capacitor c and the voltage V_f. Experiments have been made with increasing values of c (with coaxial cable at point B, Fig. 2, to preserve the pulse quality), and the pulse shapes that are obtained justify this conclusion (see Fig. 10).

Velocity of Spark Production

In accord with what has already been pointed out, one electron avalanche satisfactorily explains the fast change in the gas conductivity for a great number of them limited in amplitude by the electric energy stored in the system without regenerative processes. The time of generation of the spark already calculated can be compared with the

TABLE III. Multiplication factor of each avalanche vs distance from cathode.

Distance from cathode surface $(x)0.10^{-5}$ cm	Total multiplication at x
6	8.5×10^{3}
26	7×10^{7}
326	4×10^{9}
3676	3.5×10^{10}
3976	2×10^{13}
3996	2×10^{17}
4002	2×10^{21}

experimental values. The values of the velocity of displacement of the avalanche for high values of E/p or for a pressure of several tens of atmospheres, are not available. In order to get some idea of the order of magnitude, an extrapolation from the known values has been performed.

Various authors[8,9] have shown experimentally that the velocity is of the order of 10^8 to 3×10^8 cm/sec and is a function of E/p and not of the pressure (at least it is not appreciable).

Nesterikhin *et al.*[9] had shown that

$$v_e = 2.9\times10^6 (E/p)^{\frac{1}{2}}$$

The mean velocity has been calculated by a method similar to the one used to calculate the multiplication in one avalanche [dividing the pulse $i=i(t)$ in 10 intervals, determining the speed in each one and then finding the average]. Thus, a value $v=2.5\times10^8$ cm/sec has been obtained which gives, for $d=0.4$ mm, a time of 0.16 nsec; that is, half the time of the plasma build up and one-sixth of the whole time of the pulse.

It follows from this that the pulse characteristics will depend on the electric circuit associated with the generator, including the generator [$r=f(t)$, R and c]. Since this time is less than that required by the resistance generator to descend from 10^8 to 10^2 (0.3 nsec), the Rc of the circuit delays the time at which maximum conductivity is attained.

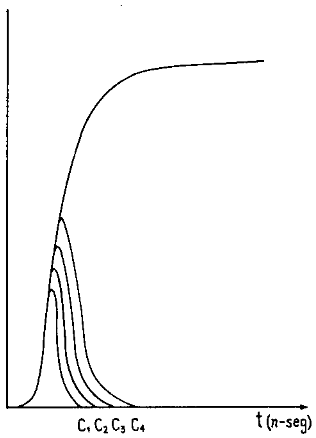

FIG. 10. Different pulses obtained with increasing values of c.

[9] Yu. E. Nesterikhin, V. S. Komel'kov, and E. Z. Meilikov, Zh. Tekhn. Fiz. 34, 40 (1964).

From the experimental results and the necessary calculation, the following scheme for pulse formation is presented.

In the first stage, up to 10% of the risetime of the pulse, the low conductivity of the gas [high $(R+r)c$], results in a slow discharge of the capacitor. The pulse $i=i(t)$ grows slowly.

The second stage, from 10 to 70% of the risetime, is due to the new shape of the surface of the mercury; the electrical resistance drops from 10^8 to 10^2 in 0.3 nsec. Without the limitations imposed by the resistance r (whose minimum value is $\sim 10^2\ \Omega$), the external resistance R and the condenser c, the risetime of the pulse must be about a half of the above given value. Working with a very low capacitance, pulses with 0.2 nsec risetimes have been obtained in good agreement with this assumption.

In the third stage, from 70 to 100% of the risetime, the resistance r decreases a little but much more slowly than before. In this time interval, the time constant is approximately 0.6 nsec ($r\simeq 80\ \Omega$, $R\simeq 50\ \Omega$, $c\simeq 4$ pF). In 0.1 nsec the potential decreases by 17%, whereas the value of r decreases some 20%. The potential divider $r+R$ produces an increase in i and V at point A of the circuit (Fig. 1) and at point B, V decreases.

The fourth stage corresponds to the decay time. This stage can be interpreted as the discharge of a capacitor c through a resistance of fixed value ($r\simeq 80\ \Omega$, $R\simeq 50\ \Omega$, $c\simeq 4$ pF). This system has a time constant of 0.52 nsec, which agrees well with the experimental value (0.5 nsec), and with the observed exponential decay. The point at which $i=0$ does not correspond to the complete discharge of the condenser but to the interruption of the spark due to the lowering of V (and hence of E) to below a certain critical value.

Influence of Mercury Vapour on the Hydrogen Ionization Process

Mercury vapour is known to increase the efficiency of the secondary electron emission process, that is, to increase the values of α.

When hydrogen gas is present, mercury atoms can act as intermediates in the electron energy transfer process and in the ionization of hydrogen. In the study of discharges in gases, it is assumed that processes with an energy higher than 5–6 eV have a low probability of occurrence since the energy that electrons acquire between two encounters is low. This is the case with the ionization of H and H_2 due to their high ionization potentials;

$$H_2 \rightarrow H_2^+ \quad 15.4\ \text{eV}, \qquad (4)$$

$$H \rightarrow H^+ \quad 10.3\ \text{eV}. \qquad (5)$$

On the other hand, the following processes have a large cross section:

$$H_2 \rightarrow 2H \qquad 4.36\ \text{eV} \qquad (6)$$

$$Hg \rightarrow Hg^*(6^3P_2) \qquad 5.47\ \text{eV} \qquad (7)$$

$$2\,Hg^*(6^3P_2) \rightarrow Hg^+ + Hg \qquad 10.44\ \text{eV} \qquad (8)$$

$$Hg^+ + H \rightarrow Hg + H^+ \qquad 10.44\ \text{eV}. \qquad (9)$$

Reaction (9) has a high probability of occurrence since it is a nearly resonant process. According to this scheme, the ionization of hydrogen through 6^3P_2 mercury-excited atoms is more probable than through process (5).[10] Although the half life of the metastable states of mercury is large compared with the duration of the pulses studied in this work, the frequency of collisions is much larger due to the high working pressure which decreases the half life of these states. The probability of processes (7)–(9) depends not only on the cross sections but also on the relative concentration of mercury in relation to hydrogen. The number of hydrogen molecules is very high. At room temperature, the vapour pressure of mercury is of the order of 10^{-3} Torr.

$$\frac{n_{Hg}}{n_H} = \frac{\text{number of Hg atoms}}{\text{number of } H_2 \text{ molecules}} = \frac{10^{-3}\ \text{Torr}}{2.5\times 10^4\ \text{Torr}} = 4\times 10^{-8}.$$

However, the mercury vapour pressure is appreciably larger than 10^{-3} Torr, due to the curvature of the mercury electrodes just before the initiation of the spark. This pressure is given by

$$p = p_0 \exp(2\sigma M/\rho RTr) = p_0 \exp(A/r)$$

where $A=(2\sigma M/RT)$, σ = surface tension, M = molecular weight, ρ = density, T = absolute temperature, and p_0 = vapour pressure of a flat surface. For mercury at 25°C, $A=5.7\times 10^{-7}$ cm (if $r\simeq 25$ Å, $p=20\ p_0$ or approximately 2×10^{-2} Torr, and $n_{Hg}/n_{H_2}\simeq 10^{-6}$). The curvature of the electrodes increases by two orders of magnitude the probability of reactions (7)–(9). Although the presence of mercury undoubtedly favors the ionization of hydrogen, it cannot be concluded from this simple calculation if there is a substantial increase in α. A more detailed theoretical and experimental study is necessary to elucidate this point.

[10] C. Kentz [Phys. Rev. **80**, 95 (1950); J. Appl. Phys. **21**, 309 (1950)], has pointed out that in the A–Hg discharge tubes, the density of the mercury metastable states 6^3P_2 and 6^3P_0 is similar or even larger than the density of the electrons. The most abundant state is the 6^3P_2.